

Manuscript No. _____

Reprints/Issues

You are entitled to a PDF for 25 hardcopies of your article. You also have the opportunity to order further issues, reprints, posters or a PDF for an unlimited number of hardcopies at the quoted rates.

Reprints of *European Journal of Organic Chemistry* articles are very popular. Whole issues, reprints, posters and high-quality PDFs are available at the rates given on a separate sheet. There is no surcharge for color reprints.

For overseas orders please note that you will receive your issues, reprints or posters by airmail unless you specifically opt for receiving them by surface mail. An appropriate surcharge will be levied to cover the higher postal rates.

Please bill me for:

Reprints

_____ (quantity)

Issues

_____ (quantity)

and send them by

surface mail courier service

Cover Posters

Posters are available of all the published covers in two sizes (see attached price list).

DIN A2 (42 x 60 cm/ 17 x 24in):

front cover back cover

DIN A1 (60 x 84 cm/ 24 x 33in):

front cover back cover

PDF (unlimited number of hardcopies)

Please bill me for

a PDF file (high resolution)

E-mail address _____

Please note that posting of the final published version on the open internet is not permitted but it can be forwarded to colleagues, added to promotion packages, etc.

★Special Offer★ If you order 200 or more reprints you will get a PDF file for half-price.

_____ reprints and a PDF file

Mail reprints/ issues/ posters to (no P.O. Boxes)

Terms of Payment

Send INVOICE to

VAT number _____

Tax-free charging can only be processed with the VAT number of the institute/company. To prevent delays with the processing, please provide us with the VAT number with this order.

Purchase Order No.: _____

Charge the CREDIT CARD

We accept



For your security please create a secured Credit Card Token which is a combination of numbers and letters that is used instead of the credit card information. Click here:

https://www.wiley-vch.de/editorial_production/index.php

TOKEN: _____

Date, Signature _____

Price List (2015)

The prices listed below are valid only for orders received in the course of 2015. Minimum order is 50 copies. Delivery time will be approximately 3 weeks after the date of publication.

If more than 500 copies are ordered, special prices are available upon request. **Single issues are available to authors at a reduced price.** The prices include mailing and handling charges (with the exception of the additional costs incurred for airmail delivery and courier services). The prices are exclusive of VAT.

Reprints, posters, and issues for overseas orders are shipped by airmail (25.00 Euro surcharge). If you would like to receive them by surface mail please indicate this on the accompanying order form (postage for shipping posters within Europe: 15.00 Euro). If you would like to use a courier service please indicate this on the order form. The cost for the courier service is 75.00 Euro.

Information regarding VAT

The charges for Reprints, Issues or Posters are considered to be "supply of goods" and therefore subject to German VAT. However, if you are an institutional customer outside Germany, the tax can be waived if you provide us with the VAT number of your company. Non-EU customers may have a VAT number starting with "EU" instead of their country code if they are registered with the EU tax authorities. If you do not have an EU VAT number and you are a taxable person doing business in a non-EU country, please provide certification from your local tax authorities confirming that you are a taxable person under local tax law. Please note that the certification must confirm that you are a taxable person and are conducting an economic activity in your country. **Note:** certifications confirming that you are a tax-exempt legal body (non-profit organization, public body, school, political party, etc.) in your country do not exempt you from paying German VAT.

Reprints	Price for orders (in Euro)					
	50 copies	100 copies	150 copies	200 copies	300 copies	500 copies
Size (pages)						
1 – 4	345.–	395.–	425.–	445.–	548.–	752.–
5 – 8	490.–	573.–	608.–	636.–	784.–	1077.–
9 – 12	640.–	739.–	786.–	824.–	1016.–	1396.–
13 – 16	780.–	900.–	958.–	1004.–	1237.–	1701.–
17 – 20	930.–	1070.–	1138.–	1196.–	1489.–	2022.–
for every additional 4 pages	147.–	169.–	175.–	188.–	231.–	315.–

Issues	22 Euro (1 copy)	PDF (high resolution)	330 Euro
Cover Posters	<ul style="list-style-type: none"> • DIN A2 (42 x 60 cm/ 17 x 24in): 38 Euro • DIN A1 (60 x 84 cm/ 24 x 33in): 48 Euro 		

★Special Offer★

If you order 200 or more reprints you will get a **PDF (high resolution)** for half-price.

The Quest for Carbenic Nitrile Imines: Experimental and Computational Characterization of a C-Amino Nitrile Imine

Cláudio M. Nunes,^{*[a]} Igor Reva^[a] Mário T. S. Rosado^[a] and Rui Fausto^[a]

Keywords: Nitrile imines / Structure elucidation / Matrix isolation / Photochemistry / Density functional calculations

A C-Amino nitrile imine has been generated as the primary photoproduct ($\lambda = 220$ nm) of 5-amino-2H-tetrazole isolated in an argon matrix at 15 K. Subsequent photochemical experiments ($\lambda = 330$ nm) demonstrated that the C-amino nitrile imine isomerizes to the corresponding three-membered-ring 1H-diazirine and decomposes to methylenimine. The experi-

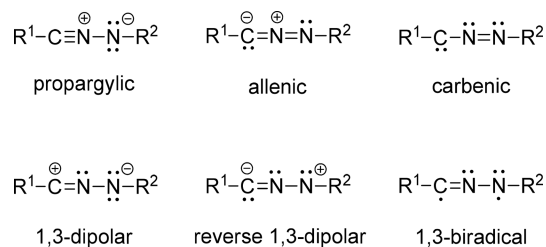
mentally observed $\nu_{\text{as}}(\text{CNN})$ absorption at 1998 cm^{-1} and a carbenic resonance structure contribution of around 20%, predicted by natural resonance theory (NRT) calculations, demonstrate that the protoproduct C-amino nitrile imine has significant carbenic character. These results pave the way to the discovery of carbenic nitrile imines.

Introduction

Nitrile imines ($\text{R}'\text{-CNN-R}''$) are reactive intermediates known as 1,3-dipoles that participate in 1,3-cycloaddition reactions; they are versatile reactions ■■ ((=>AUTHOR: "reactions" or "reagents"?)) ■■ used in drug discovery, biological chemistry, and materials and synthetic chemistry.^[1–5] One interesting example of the use of nitrile imines is the light-induced click cycloaddition reaction promoted by the decomposition of tetrazoles.^[6,7] This powerful reaction method has been applied to the in vivo labeling of proteins and cells, nanomaterial functionalization, and other promising applications.^[8–12]

Geometric and electronic structures are known to play an important role in the regiochemistry and reactivity of 1,3-dipolar species.^[1,2,13–15] Concerning nitrile imines, it is known that they exist as a single minimum on the potential energy surface,^[16] which is best described by different resonance structures with different weights (Scheme 1). Usually, one of the resonance structures predominates over the others and is used to describe the geometry, bonding, and reactivity of that particular nitrile imine.^[17,18] Nevertheless, the structural nature of nitrile imines has been a subject of continuing debate, and it is not yet completely understood. For instance, using ab initio calculations up to the QCISD level, the parent nitrile imine H-CNN-H was found to have a nonplanar geometry and therefore assumed to be of the allenic type. The hypothetical planar propargylic-type structure, characterized by a linear HCN fragment and a CN triple bond, was found to be the transition state be-

tween two equivalent allenic forms.^[19] Alternatively, a combination of DFT calculations and natural resonance theory (NRT) analysis has shown that a complete description of nitrile imines requires a combination of four major resonance structures: Propargylic, allenic, 1,3-dipolar, and carbenic.^[20] Different ways to describe the geometric and electronic structures of the parent nitrile imine have also been reported by means of valence bond (VB) calculations.^[13,21]



Scheme 1. Different resonance forms that can represent the structure of a nitrile imine.

Several nitrile imines have been captured in low-temperature matrices and characterized spectroscopically.^[16–18,22–28] Substituents were found to have a significant effect on the structural characteristics of nitrile imines. This is particularly noticeable by the CNN antisymmetric stretching IR absorption of the nitrile imine moiety appearing over a wide range of frequencies ($2000\text{--}2250\text{ cm}^{-1}$).^[17,18] Nitrile imines with an IR absorption above 2150 cm^{-1} , such as Ph-CNN-SiMe₃, Ph-CNN-Ph, and boryl-CNN-boryl, have been described as mainly propargylic, whereas those with an IR absorption between $2000\text{--}2100\text{ cm}^{-1}$, such as H-CNN-H, Ph-CNN-H, Ph-CNN-Me, H-CNN-Ph, and Ph₃C-CNN-CPh₃, have been described as mainly allenic.^[17]

In addition, theoretical studies have indicated that substituents bearing a lone-electron pair should increase the importance of the carbenic resonance structure of nitrile

[a] CQC, Department of Chemistry, University of Coimbra, 3004-535 Coimbra, Portugal
E-mail: cmnunes@qui.uc.pt
<https://woc.uc.pt/quimica>

Supporting information and ORCID(s) from the author(s) for this article are available on the WWW under <http://dx.doi.org/10.1002/ejoc.201501153>.

FULL PAPER

71 imines.^[20,29,30] For instance, Bégue and Wentrup have theo-
 retically investigated different amino-, hydroxy-, and fluoro-
 substituted nitrile imines (R–CNN–H, H–CNN–R, and R–
 CNN–R; R = NH₂, OH, and F) and predicted that some of
 the studied molecules should exhibit carbenic character.^[30]
 76 These postulated carbenic nitrile imines were predicted to
 lack the intense IR absorption in the 2000–2250 cm⁻¹ re-
 gion that characterizes other nitrile imines. Instead, moder-
 ate IR intensities below 2000 cm⁻¹ are expected for carbenic
 nitrile imines.^[30]

81 A recent preliminary report concerning the characteriza-
 tion of two disubstituted amino nitrile imine derivatives
 seems to attest the lack of the intense IR absorption in the
 2000–2250 cm⁻¹ region, but this also made their experimen-
 tal identification difficult.^[24] Therefore, the question still re-
 mains as to whether nitrile imines of predominantly carbenic
 86 type can be generated and characterized. Addressing
 the quest for carbenic nitrile imines, herein we report, for
 the first time, the experimental and computational charac-
 terization of a C-amino nitrile imine. The $\nu_{\text{as}}(\text{CNN})$ absorp-
 tion below 2000 cm⁻¹ and a carbenic resonance structure
 91 contribution of around 20%, predicted by natural reso-
 nance theory (NRT) calculations, demonstrate that the C-
 amino nitrile imine has significant carbenic character.

Results

96 Tautomeric Equilibria in 5-Monosubstituted Tetrazoles –
 Potential Precursors of Carbenic Nitrile Imines

We started to address the quest for the experimental gen-
 eration of carbenic nitrile imines by considering the study
 of the simplest amino and hydroxy C-monosubstituted

101 nitrile imines (R–CNN–H).^[31] An efficient way to generate
 and capture unstable nitrile imines is to photolyze a tetraz-
 ole precursor under low-temperature matrix-isolation con-
 ditions.^[16,17,23,28] Tetrazoles can adopt different tautomeric
 forms, but only the 2*H*-tetrazole forms can give a direct
 access to nitrile imines.^[16,17,23,28] Therefore, to ascertain if
 5-amino- and 5-hydroxytetrazole are suitable candidates to
 106 generate the corresponding nitrile imines, they were struc-
 turally characterized theoretically.

Tables 1 and 2 show the relative energies calculated at the
 B3LYP/6-311++G(d,p) and CBS-QB3 levels of theory for
 isomers of 5-amino- and 5-hydroxytetrazole, respectively. 111
 For 5-aminotetrazole, the results indicated the 5-amino-2*H*-
 tetrazole tautomer form (**A1**) to be the most stable, with the
 1*H*-tetrazole tautomer (**A2**) found to be around 13 kJ mol⁻¹
 higher in energy (Table 1). All the imino tautomeric forms
 (**I1–I3**) have very high predicted energies (over 50 kJ mol⁻¹). 116
 For 5-hydroxytetrazole, the computations indicated that the
 oxo form 1*H*-tetrazol-5(4*H*)-one (**O1**) is the most stable
 tautomer. In comparison, the 5-hydroxy forms of 1*H*-
 tetrazole (**H1** and **H2**) ■■ ((=<=AUTHOR: In Table 2, 1*H*-
 tetrazole is represented as H3 and H4, and 2*H*-tetrazole is 121
 represented as H1 and H2; please check!)) ■■ and of 2*H*-
 tetrazole (**H3** and **H4**) are very high in energy (over
 27 kJ mol⁻¹).

It can be anticipated from the calculations that only the
 5-amino-2*H*-tetrazole (**A1**) and 1*H*-tetrazol-5(4*H*)-one (**O1**) 126
 forms would be present in the sublimated vapors of 5-ami-
 no- and 5-hydroxytetrazole, respectively. All other tauto-
 mers would have negligible populations in the gas-phase
 equilibrium prior to deposition of the matrix. Therefore, the
 compound that is nominally called 5-hydroxytetrazole in 131
 practice will exist in the matrix as 5-oxotetrazole **O1**, and

Table 1. Relative zero-point-corrected energies [kJ mol⁻¹] calculated at the B3LYP/6-311++G(d,p) and CBS-QB3 levels of theory for isomers of 5-aminotetrazole.^[a]

Structure					
Name	A1	A2	I1	I2	I3
B3LYP	0.0	13.3	51.2	121.5	136.2
CBS-QB3	0.0	13.0	60.4	134.3	147.0

[a] In the names of the structures, **A** stands for “amino”, **I** stands for “imino”, and the numeric value corresponds to the order of the relative energies.

Table 2. Relative zero-point-corrected energies [kJ mol⁻¹] calculated at the B3LYP/6-311++G(d,p) and CBS-QB3 levels of theory for isomers of 5-hydroxytetrazole.^[a]

Structure						
Name	O1	H1	H2	H3	H4	O2
B3LYP	0.0	41.4	45.1	47.9	74.2	92.5
CBS-QB3	0.0	27.4	31.0	35.1	59.3	97.3

[a] In the names of the structures, **O** stands for “oxo”, **H** stands for “hydroxy”, and the numeric value corresponds to the order of the relative energies.

its photochemistry will not lead to the formation of the corresponding *C*-hydroxy nitrile imine. In contrast, 5-aminotetrazole will exist in the 2*H*-tautomeric form **A1**, which is a suitable precursor to generate the corresponding nitrile imine. Therefore, the present study focused on the generation and characterization of the previously unknown *C*-amino nitrile imine.

Infrared Spectrum of Matrix-Isolated 5-Aminotetrazole

The experimental IR spectrum of monomeric 5-aminotetrazole (**1**) isolated in an argon matrix at 15 K and the simulated theoretical IR spectra of 5-amino-2*H*-tetrazole (**1''**) and 5-amino-1*H*-tetrazole (**1'**) are shown in Figure 1. The particularly good agreement between the experimental and theoretical IR spectra of 5-amino-2*H*-tetrazole (**1''**) indicates that only the 2*H*-tautomer is present in the matrix.^[32] This is most clear in the 3600–3400 cm⁻¹ region; three bands observed at 3528, 3478, and 3432 cm⁻¹ have unequivocally been assigned to the NH stretching modes predicted for 2*H*-tetrazole (**1''**) at 3506 [ν_{as}(NH₂)], 3464 [ν(N–H)], and 3406 cm⁻¹ [ν_s(NH₂)]. In contrast, the calculated IR spectrum of 1*H*-tetrazole (**1'**) exhibits three vibrational modes at 3479 [ν_{as}(NH₂)], 3472 [ν(N–H)], and 3388 cm⁻¹ [ν_s(NH₂)], the frequency and intensity patterns of which are not compatible with the most intense bands observed experimentally (see also Figure S1 in the Supporting Information). The analysis of the fingerprint range of the IR spectrum also supports the conclusion about the absence of the 1*H*-tetrazole (**1'**) form in the matrix.

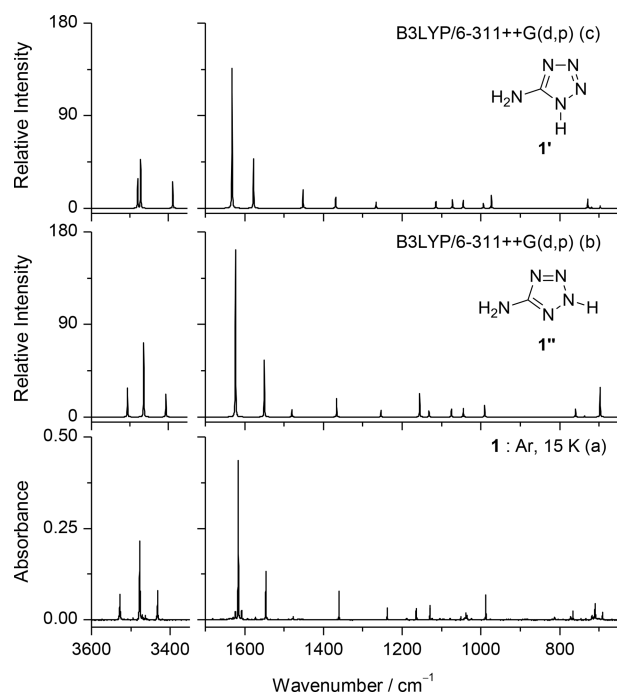


Figure 1. (a) Experimental IR spectrum of 5-aminotetrazole (**1**) isolated in an argon matrix at 15 K. IR spectra of (b) 5-amino-2*H*-tetrazole (**1''**) and (c) 5-amino-1*H*-tetrazole (**1'**) simulated at the B3LYP/6-311++G(d,p) level of theory. Details of the simulated spectra are given in the Exp. Sect.

Photochemistry of Matrix-Isolated 5-Aminotetrazole

The photochemistry of matrix-isolated 5-amino-2*H*-tetrazole (**1''**) was induced by using monochromatic UV light with λ = 220 nm, chosen to match the absorption maximum of **1** [UV/Vis (ACN): λ_{max} ≈ 218 nm; Figure S2 in the Supporting Information]. Figure 2 shows the result after a total irradiation time of 120 s, when around 50% of **1''** was consumed and five different products, labeled as **2–6**, were formed (see also Figure S3). The bands due to photoproduct **2** (1998 and ca. 1602 cm⁻¹) appear immediately after the first seconds of irradiation and stop increasing after 120 s, whereas photoproducts **3** (1640 cm⁻¹), **4** (1823 cm⁻¹), **5** (2111 cm⁻¹), and **6** (2031 cm⁻¹) continue to accumulate in the matrix upon further irradiation. This observation indicates that **2** is most likely a primary photoproduct of **1''** that is subsequently transformed into the other photoproduct(s). Because the first step in the photochemical reaction of other 2*H*-tetrazoles was found to lead to nitrile imines by extrusion of N₂,^[16,17,23] it is conceivable that photoproduct **2** corresponds to the *C*-amino nitrile imine.

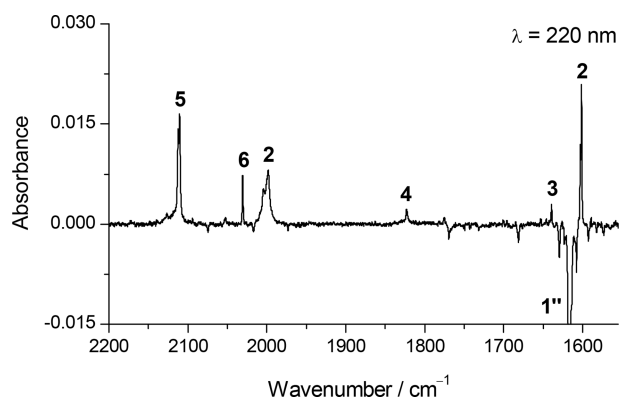


Figure 2. Experimental difference IR spectrum obtained as the spectrum after UV irradiation at λ = 220 nm (120 s, ca. 2 mW) of 5-amino-2*H*-tetrazole (**1''**) isolated in an argon matrix at 15 K “minus” the spectrum of **1''** before irradiation. The negative bands are due to consumed **1''**, the positive bands labeled **2–6** are the most characteristic bands of the generated photoproducts.

To clearly identify the photoproducts, additional data concerning their IR spectral signatures and their photochemical behavior were obtained. This was achieved by performing subsequent irradiations using longer wavelengths, that is, under conditions under which the tetrazole **1''** precursor does not react, but some of the photoproducts can be consumed.^[33]

Identification of Products **2–6** from the Irradiation of 5-Aminotetrazole

By applying subsequent irradiations, starting at λ = 400 nm and gradually decreasing the wavelength, it was found that irradiation at around 330 nm started to affect the bands of the photoproducts.^[34] The first stage of the irradiation under these conditions during 8 min resulted in the complete consumption of **2** and an increase in **3–5** (Figure 3). From a comparison of the experimental and calcu-

FULL PAPER

201

lated IR spectra, photoproduct **2** is clearly identified as the *C*-amino nitrile imine. Particularly characteristic is the band observed at 1998 cm⁻¹, which corresponds to the antisymmetric stretching mode $\nu_{\text{as}}(\text{CNN})$ predicted at 1966 cm⁻¹. As mentioned before, this vibration is particularly sensitive to the geometric and electronic characteristics of a particu-

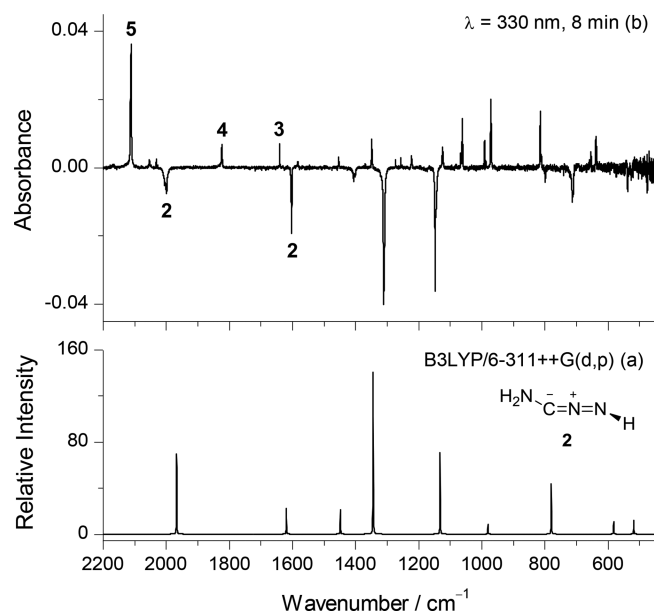


Figure 3. (a) IR spectrum of the *C*-amino nitrile imine **2** simulated at the B3LYP/6-311++G(d,p) level of theory. (b) Experimental difference IR spectrum showing changes after irradiation at $\lambda = 330$ nm (8 min, 35 mW) in an argon matrix (subsequent to the initial irradiation of **1''** at $\lambda = 220$ nm; see Figure 2). The negative bands are due to the consumed photoproduct **2**, assigned to the *C*-amino nitrile imine **2**. The positive bands are due to photoproducts **3–5**.

lar nitrile imine. We return to this subject in the next section. Other strong absorption bands of **2** were observed at around 1602, 1310, and 1147 cm⁻¹, in good correspondence with the most intense vibrational modes predicted for the *C*-amino nitrile imine at 1618 [$\delta(\text{NH}_2)$], 1343 [$\delta(\text{NNH})$], and 1131 [$\gamma(\text{NH}_2)$] cm⁻¹. The comprehensive assignments of 11 out of the 12 vibrations expected for the mid-IR spectrum of the *C*-amino nitrile imine **2** are given in Table 3.

In the experimental difference IR spectrum presented in Figure 3b, which shows the increase in bands due to photoproducts **3–5** during the irradiation at $\lambda = 330$ nm, bands due to methylenimine ($\text{HN}=\text{CH}_2$) were clearly identified and unequivocally assigned to photoproduct **3**. The identification was based on a previously reported IR spectrum of methylenimine generated by photolysis of methyl azide isolated in an argon matrix.^[35] The most characteristic IR band of **3** is observed at 1640 cm⁻¹ and corresponds to the $\nu(\text{C}=\text{N})$ stretching mode. Other strong bands observed at around 1347, 1123, and 1060 cm⁻¹ are also distinctive of the IR spectrum of **3** in an argon matrix. With the exception of the $\nu(\text{NH})$ stretching mode estimated at 3261 cm⁻¹, which has a very low predicted IR intensity, all the remaining eight vibrational modes of methylenimine were identified in agreement with previous experimental data and with its calculated IR spectrum (Table 4).

Jacox and Milligan reported that during the photogeneration of methylenimine from methyl azide, the compound partially decomposes into hydrogen isocyanide (HNC).^[35,36] Indeed, the photoproduct **6**, which was simultaneously produced with photoproduct **3** (methylenimine) during the irradiation of **1''** at $\lambda = 220$ nm, was unequivocally identified as HNC. The bands of **6** observed in this work at 3576 (s), 2031 (m), and 537 (br.) cm⁻¹ are in good

Table 3. Experimental IR spectral data (argon matrix at 15 K), B3LYP/6-311++G(d,p)-calculated vibrational frequencies (ν), absolute IR intensities (A^{th}), and vibrational assignments of the *C*-amino nitrile imine **2**.

Ar matrix ^[a] ν [cm ⁻¹]	<i>I</i>	ν [cm ⁻¹]	Calcd. ^[b] A^{th} [km mol ⁻¹]	Approximate assignment ^[c]
3532/3527/3522	m	3514	79.7	$\nu_{\text{as}}(\text{NH}_2)$
3408/3404/3399	w	3355	2.9	$\nu_{\text{s}}(\text{NH}_2)$
3177	vw	3170	4.3	$\nu(\text{NH})$
2004/1998	m	1966	124.7	$\nu_{\text{as}}(\text{CNN})$
1603/1601	m	1618	36.6	$\delta(\text{NH}_2)$
1405/1400	w	1447	40.3	$[\nu(\text{NN}) - \nu(\text{CN})] + \delta(\text{NNH})$
1310	s	1343	239.8	$\delta(\text{NNH}) - [\nu(\text{NN}) - \nu(\text{CN})]$
1147	s	1131	115.4	$\gamma(\text{NH}_2)$
989	o	980	13.1	$\nu(\text{NN}) + \nu(\text{CN})$
797 or 712/710	w/m	779	69.3	$\tau(\text{NH})$
537	m	581	17.5	$\tau(\text{NH}_2)$
[d]	–	517	21.4	$\tau(\text{NCNN}) + [\delta(\text{NCN}) + \delta(\text{NNC})]$
n.i.	–	286	45.9	$\delta(\text{NCN}) - \delta(\text{NNC})$
n.i.	–	225	186.5	$\omega(\text{NH}_2)$
n.i.	–	154	43.2	$[\delta(\text{NCN}) + \delta(\text{NNC})] - \tau(\text{NCNN})$

[a] The *C*-amino nitrile imine **2** was generated by irradiation of 5-amino-2*H*-tetrazole (**1''**) at $\lambda = 220$ nm in an argon matrix. Experimental spectra were not recorded below 400 cm⁻¹. n.i. = not investigated. Experimental intensities are presented in qualitative terms: s = strong, m = medium, w = weak, vw = very weak, and o = overlap. [b] Scaled \blacksquare (\llcorner =AUTHOR: Ok or "calculated"? Also in Table 4)) \blacksquare B3LYP/6-311++G(d,p) frequencies. [c] Assignments made by inspection of Chemcraft animations: ν = stretching, δ = bending, γ = rocking, ω = wagging, τ = torsion, s = symmetric, and as = antisymmetric. Signs "+" and "-" designate combinations of vibrations occurring in the "syn" ("++") and "anti" ("--") phases. [d] The low signal/noise ratio in this region precludes the identification of this band.

Table 4. Comparison of the experimental IR spectrum of photoproduct **3** (argon matrix at 15 K) with a previously reported IR spectrum of methylenimine (argon matrix at 4 K) and with B3LYP/6-311++G(d,p)-calculated vibrational frequencies (ν), absolute infrared intensities (A^{th}), and vibrational assignment of methylenimine **3**.

This work ^[a]		Previous work ^[b]		ν [cm^{-1}]	Calculated ^[c] A^{th} [km mol^{-1}]	Sym.	Approximate assignment ^[d]
ν [cm^{-1}]	I	ν [cm^{-1}]	I				
—	—	—	—	3261	1.5	A'	$\nu(\text{NH})$
3039/3035	vw	3035	m	3050	32.6	A'	$\nu_{\text{as}}(\text{CH}_2)$
2924	m	2926	s	2951	52.7	A'	$\nu_{\text{s}}(\text{CH}_2)$
1640	s	1641	s	1673	24.9	A'	$\nu(\text{C}=\text{N})$
1453/1452	m	1453	s	1463	6.8	A'	$\delta(\text{CH}_2)$
1348/1346	s	1348	s-vs	1343	35.0	A'	$\gamma(\text{CH}_2) - \delta(\text{HNC})$
1123	s	1123	vs	1138	47.4	A''	$\tau(\text{HN}=\text{CH}_2)$
1066/1064	m	1063	s	1083	17.7	A''	$\omega(\text{CH}_2)$
1061/1059	s	1059	s	1052	34.4	A'	$\gamma(\text{CH}_2) + \delta(\text{HNC})$

[a] Methylenimine **3** generated in this study in an argon matrix. [b] Methylenimine **3** generated by mercury arc lamp irradiation of methyl azide in an argon matrix.^[35] Experimental intensities are presented in qualitative terms: vs = very strong, s = strong, m = medium, w = weak, and vw = very weak. ■■ ((=>AUTHOR: What does "s-vs" represent?)) ■■ [c] Scaled B3LYP/6-311++G(d,p) frequencies. [d] Assignments made by inspection of Chemcraft animations: ν = stretching, δ = bending, γ = rocking, ω = wagging, τ = torsion, s = symmetric, and as = antisymmetric. Signs "+" and "-" designate combinations of vibrations occurring in the "syn" ("+") and "anti" phases ("-").

agreement with the previously reported bands at 3583, 2032, and 535 cm^{-1} for HNC isolated in an argon matrix at 4 K^[36] and also with the B3LYP-calculated frequencies for this species.^[37]

241 After the complete consumption of the *C*-amino nitrile imine **2**, it was found in a second stage of irradiations at $\lambda = 330$ nm that **4** was converted into **5** (Figure 4). With the

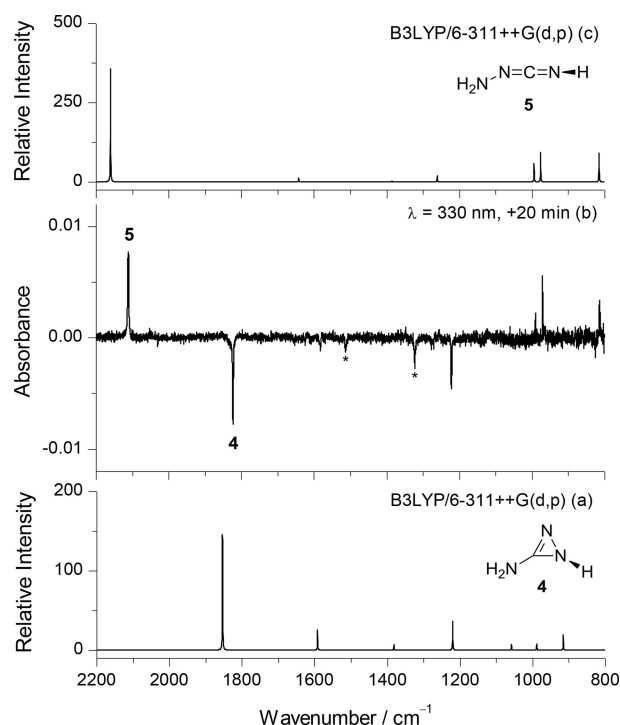
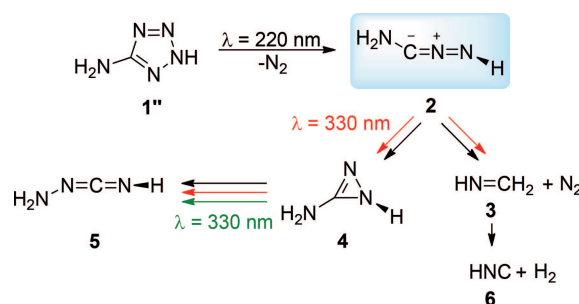


Figure 4. (a) IR spectrum of 1*H*-diazirine **4** simulated at the B3LYP/6-311++G(d,p) level of theory. (b) Experimental difference IR spectrum showing changes after irradiation at $\lambda = 330$ nm for 20 min (35 mW; subsequent to the irradiation at $\lambda = 330$ nm for 8 min; see Figure 3). The negative bands are due to the consumed photoproduct **4**, assigned to 1*H*-diazirine **4**. The asterisks indicate unidentified bands at 1513 and 1322 cm^{-1} . The positive bands are due to the growing photoproduct **5** assigned to carbodiimide **5**. (c) IR spectrum of carbodiimide **5** simulated at the B3LYP/6-311++G(d,p) level of theory.

support of calculated IR spectra, the photoproducts **4** and **5** were identified as 1*H*-diazirine and carbodiimide derivatives, respectively, isomeric of **2**. The strongest IR vibrational modes of 1*H*-diazirine **4** were predicted to be at 1853 [$\nu(\text{C}=\text{N})$, particularly characteristic], 1592 [$\delta(\text{NH}_2)$], and 1220 [$\delta(\text{CNH})$] cm^{-1} and assigned to the bands observed at 1823, 1582, and around 1221 cm^{-1} , respectively, in the experimental difference spectrum ■■ ((=>AUTHOR: Change ok? Also below!)) ■■ (Figure 4a,b). For carbodiimide **5**, the calculations predicted strong IR modes at 2160 [$\nu_{\text{as}}(\text{NCN})$; particularly characteristic], 994 [$\omega(\text{NH}_2)$], 976 [$\delta(\text{CNH})$], and 815 [$\nu(\text{NN})$] cm^{-1} , which unequivocally correspond to the bands observed at 2111, 991, 971, and 814 cm^{-1} , respectively, in the experimental difference spectrum (Figure 4b,c).

Mechanistic Discussion of the Photochemistry of Matrix-Isolated 5-Aminotetrazole

261 The experimental results obtained for the photochemistry of matrix-isolated 5-amino-2*H*-tetrazole (**1''**) is shown in Scheme 2. Irradiation at $\lambda = 220$ nm leads to the forma-



Scheme 2. Summary of experimental observations in the UV-induced photochemistry of 5-amino-2*H*-tetrazole (**1''**) isolated in an argon matrix: Generation of the *C*-amino nitrile imine **2** and its photochemical transformation into **5** via **4** and decomposition to **3**. The colors of the arrow are related to different wavelengths and irradiation stages: $\lambda = 220$ nm (black), $\lambda = 330$ nm first stage (red), and $\lambda = 330$ nm second stage (green).

FULL PAPER

tion of the *C*-amino nitrile imine **2**, methylenimine **3**, 1*H*-diazirine **4**, carbodiimide, and hydrogen isocyanide **6**. Subsequent irradiation at $\lambda = 330$ nm leads to the consumption of **2** and increase in the populations of **3–5**. This observation indicates that two different pathways are involved in the photochemistry of the *C*-amino nitrile imine **2**: (1) Rearrangement to the 4 π -electron three-membered-ring 1*H*-diazirine **4** and (2) decomposition involving hydrogen shifts and CN bond cleavage to give methylenimine **3** and N₂.

Concerning pathway (1), it shall be recalled that during the first stage of irradiation at $\lambda = 330$ nm, the transformation of **2** is accompanied by an increase in both **4** and **5**. We hypothesize that the *C*-amino nitrile imine **2** isomerizes to 1*H*-diazirine **4** concomitantly with the transformation of **4** into carbodiimide **5**. Under such circumstances the reaction of **2** to **4** would be faster than the reaction of **4** to **5**, in accordance with the predicted difference in the UV/Vis absorptions of these two species (see Figure S4 in the Supporting Information). In fact, as mentioned above, after **2** had been completely consumed, the second stage of irradiation at $\lambda = 330$ nm leads to the isomerization of **4** to **5**. This is good evidence that the *C*-amino nitrile imine **2** photoisomerizes to 1*H*-diazirine **4**, which in turn isomerizes to carbodiimide **5**, following the same trend proposed in our previous work on the photochemistry of matrix-isolated *C*-methyl and *C*-phenyl nitrile imines.^[16,23]

Concerning pathway (2), it should be noted that the formation of methylenimine **3** was observed in the first stage of irradiation at $\lambda = 330$ nm, and could in principle result from either the consumption of the *C*-amino nitrile imine **2** or 1*H*-diazirine **4**. However, its formation via 1*H*-diazirine **4** can clearly be ruled out, because it is not observed during the second stage of irradiation at $\lambda = 330$ nm, in which only **4** is consumed. Interestingly, the formation of methylenimine **3** via the *C*-amino nitrile imine **2** seems to be a new route in the photochemistry of nitrile imines.

Mechanistically, we postulate that the first step in the decomposition of **2** (H₂N–CNN–H) involves a [1,3] hydrogen shift from the imine group to the carbon atom. Such hydrogen-atom migration may occur concomitantly with N₂ extrusion leading to an aminocarbene intermediate (H₂N–C–H), which then rearranges to methylenimine by a [1,2] hydrogen shift from the N atom to the C atom. Alternatively, the [1,3] hydrogen shift may take place initially to form a diazo intermediate [H₂N–C(H)=N₂], which sub-

sequently releases the N₂ molecule to form the aminocarbene intermediate (H₂N–C–H), which then rearranges to methylenimine. Although the diazo compound was not experimentally detected, the last mechanism could not be ruled out, because it is well known that diazo compounds readily release N₂ when subjected to experimental conditions similar to those used in the present study.^[38,39] In turn, the elusive nature of the aminocarbene, even in a low-temperature matrix, is also not surprising. For instance, the parent hydroxycarbene (HO–C–H) is known to rearrange by a [1,2] hydrogen shift to formaldehyde through quantum tunneling in an argon matrix.^[40]

Whatever the mechanism for decomposition of the nitrile imine to methylenimine (that is, a concerted [1,3] hydrogen shift and N₂ release or consecutive [1,3] hydrogen shift and N₂ release via a diazo intermediate), the initial [1,3] hydrogen shift from the imine group to the carbon atom is always favored by an increase in the electron density at the carbon atom to which the hydrogen atom migrates. Hence, it seems rather probable that the carbenic character of **2** is crucial to open up the decomposition route to methylenimine **3**. It can also be suggested that this might be a more general reactivity pattern distinguishing carbenic-type nitrile imines from allylic- or propargylic-type nitrile imines (bearing a lower electron density at the carbon atom).

Nature of the *C*-Amino Nitrile Imine – Geometric and Electronic Structure Analysis

To gain more insight into the nature of the *C*-amino nitrile imine **2** (H₂N–CNN–H), its geometry and electronic structure were analyzed with the aid of theoretical calculations. The parent nitrile imine (H–CNN–H) and *C*-methyl nitrile imine (H₃C–CNN–H) were also investigated to better understand the substituent effect on the carbon atom of nitrile imines.^[41] Previous theoretical studies by Bégué and Wentrup indicated the need for post-Hartree–Fock calculations, such as coupled-cluster (CC) methods, to correctly assess the electronic structures of nitrile imines.^[30] Thus, the CCSD(T) method was used in the present investigation with the 6-311++G(d,p) basis set, in addition to the standard B3LYP calculations with the same basis set.

Table 5 presents selected optimized geometric parameters as well as experimental and calculated vibrational fre-

Table 5. CCSD(T)/6-311++G(d,p) (**bold**) and B3LYP/6-311G++(d,p) (*italic*) selected optimized geometric parameters, calculated and experimental vibrational frequencies of the $\nu_{\text{as}}(\text{CNN})$ mode for nitrile imines R–CNN–H (R = NH₂, H, and CH₃).^[a]

Nitrile imine	$r(\text{CN})$ [Å]	$r(\text{NN})$ [Å]	$\theta(\text{RCN})$ [°]	$\theta(\text{CNN})$ [°]	$\nu_{\text{as}}(\text{CNN})_{\text{cal.}}^{[b]}$ [cm ⁻¹]	$\nu_{\text{as}}(\text{CNN})_{\text{exp.}}^{[c]}$ [cm ⁻¹]
H ₂ N–CNN–H	1.226 <i>1.217</i>	1.267 <i>1.255</i>	129.9 <i>132.8</i>	158.6 <i>157.3</i>	1993 <i>1966 (125)</i>	1998 ^[d]
H–CNN–H	1.208 <i>1.190</i>	1.256 <i>1.242</i>	128.9 <i>133.0</i>	167.6 <i>169.5</i>	2058 <i>2085 (416)</i>	2033 ^[e]
H ₃ C–CNN–H	1.201 <i>1.181</i>	1.267 <i>1.256</i>	136.4 <i>144.5</i>	168.3 <i>170.0</i>	2129 <i>2184 (423)</i>	2138 ^[f]

[a] The $\nu_{\text{as}}(\text{CNN})$ frequency value is not scaled for CCSD(T)/6-311++G(d,p) calculations and is scaled by 0.98 for B3LYP/6-311++G(d,p) calculations. [b] Calculated absolute IR intensities [kmol⁻¹] are given in parentheses. [c] Molecules isolated in argon matrices. [d] This work. [e] See ref.^[28] [f] See ref.^[23]

351 frequencies of the $\nu_{\text{as}}(\text{CNN})$ mode for the three nitrile imines
 356 obtained by both methods of calculation. Only a single
 361 minimum of C_1 symmetry was found on the potential
 energy surface of all three nitrile imines (Figure 5). The calcu-
 lated geometric parameters show a shorter CN bond and a
 larger RCN bond angle for the *C*-methyl nitrile imine. A
 longer CN bond and a larger deviation from linearity of
 the CNN angle are observed for the *C*-amino nitrile imine.
 Considering the idealized structures presented in Scheme 3,
 the geometrical data appear to indicate an increase in prop-
 argylic character upon methyl substitution ($\text{H}_3\text{C}-\text{CNN}-\text{H}$)
 and an increase in carbenic character upon amino substitu-
 tion ($\text{H}_2\text{N}-\text{CNN}-\text{H}$), although the geometries of the three
 nitrile imines seem to be closer to an allenic-type molecule.

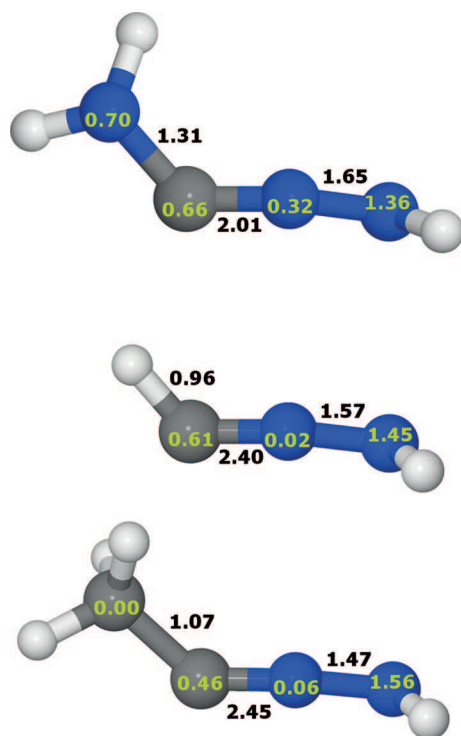
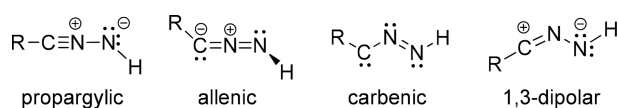


Figure 5. Optimized CCSD(T)/6-311++G(d,p) geometries of the nitrile imines $\text{R}-\text{CNN}-\text{H}$ ($\text{R} = \text{NH}_2$, H and CH_3), natural bond orders (black), and nonbonded natural electron populations (lime) from NRT calculations. Atom colors: C (grey), N (blue), and H (white).



Scheme 3. Idealized limiting geometric structures of the nitrile imines.

366 The data obtained by this theoretical analysis agrees with
 371 the experimental IR data. Taking as reference the parent
 nitrile imine, with $\nu_{\text{as}}(\text{CNN})$ at 2033 cm^{-1} , methyl substi-
 tution leads to an increase in $\nu_{\text{as}}(\text{CNN})$ to 2138 cm^{-1} , whereas
 amino substitution leads to a decrease in $\nu_{\text{as}}(\text{CNN})$ to
 1998 cm^{-1} . As mentioned before, frequencies of $\nu_{\text{as}}(\text{CNN})$
 between $2000\text{--}2100\text{ cm}^{-1}$ are known to characterize allenic-

type nitrile imines and those above 2150 cm^{-1} are found for
 propargylic-type nitrile imines;^[16–18] $\nu_{\text{as}}(\text{CNN})$ modes be-
 low 2000 cm^{-1} and with moderate IR intensities are pre-
 dicted for nitrile imines with significant carbenic charac-
 ter.^[30]

Calculations using natural resonance theory (NRT) were
 performed on the three considered nitrile imines ($\text{R} = \text{H}$,
 CH_3 , NH_2) to determine the weights of the important reso-
 nance hybrids (more details are given in the Exp. Sect.).
 The results of the NRT analysis using the wavefunctions
 calculated at the CCSD(T)/6-311++G(d,p) level for the
 fully optimized geometries of the three nitrile imines are
 given in Table 6. Only resonance hybrids with contributions
 greater than 2% are presented. Figure 5 shows bond orders
 and nonbonded lone-pair electron populations obtained
 from these calculations. The corresponding results calcu-
 lated at the B3LYP level of theory are given in the Support-
 ing Information.

Table 6. Resonance structure contribution [%] from NRT analysis calculated at the CCSD(T)/6-311+G(d,p) level of theory for nitrile imines $\text{R}-\text{CNN}-\text{H}$ ($\text{R} = \text{NH}_2$, H , and CH_3).

Nitrile imine	Resonance structures			
	$\text{R}-\text{C}\equiv\ddot{\text{N}}-\ddot{\text{N}}-\text{H}$ propargylic	$\text{R}-\overset{\ominus}{\text{C}}=\overset{\oplus}{\text{N}}=\ddot{\text{N}}-\text{H}$ allenic	$\text{R}-\overset{\ominus}{\text{C}}-\overset{\oplus}{\text{N}}=\ddot{\text{N}}-\text{H}$ carbenic	$\text{R}-\overset{\oplus}{\text{C}}=\overset{\ominus}{\text{N}}-\ddot{\text{N}}-\text{H}$ 1,3-dipolar
$\text{H}_2\text{N}-\text{CNN}-\text{H}$	23	40	19	10
$\text{H}-\text{CNN}-\text{H}$	43	49	–	–
$\text{H}_3\text{C}-\text{CNN}-\text{H}$	52	32	–	–

The results of the NRT analysis corroborate the previous
 interpretation based on the geometrical parameters and vi-
 brational frequencies of the CNN moiety of nitrile imines.
 The parent nitrile imine ($\text{R} = \text{H}$) is described in terms of
 two resonance hybrids; the major contributor with a weight
 of 49% corresponds to the allenic hybrid and the other con-
 tributor with 43% weight corresponds to the propargylic
 hybrid. Upon methyl substitution, the propargylic reso-
 nance hybrid becomes the major contributor with 52%
 weight; a significant 32% weight of the allenic hybrid also
 contributes to the description of the *C*-methyl nitrile imine.
 Upon amine substitution, the contribution of the propargy-
 lic hybrid decreases considerably to 23% and, although the
 allenic hybrid is the major contributor with 40% weight, a
 new important contribution from the carbenic hybrid with
 around 20% weight characterizes the *C*-amino nitrile imine
 (with also ca. 10% of the 1,3-dipole hybrid).

The electronic structure analysis agrees well with the data
 of natural bond orders and nonbonded natural electron
 populations also obtained from NRT calculations (Fig-
 ure 5). For instance, the lone-pair occupancy of the nitrile
 imine C atom increases on going from methyl (0.48e) to
 amino substitution (0.66e; along with a decrease in the CN
 bond order and an increase in the NN bond order), which
 reflects the decrease in the contribution of the propargylic
 character and the increase in both the allenic and carbenic
 character, both characterized by the existence of lone-pair
 electrons of this carbon atom. The occupancy of the lone-
 pair of the terminal N atom of the CNN fragment decreases

FULL PAPER

on going from methyl (1.56*e*) to amino substitution (1.36*e*), which also reflects the decrease in the propargylic character, characterized by the existence of negative charge of this nitrogen atom. Finally, the lone-pair population of the central N atom of the CNN fragment was found to be only relevant in the *C*-amino nitrile imine (0.32*e*). Interestingly, this seems to reflect the importance of the carbenic contribution (ca. 20%) in the *C*-amino nitrile imine (and possibly also some degree of the 1,3-dipolar contribution). The fact that the *C*-amino nitrile imine shows significant carbenic character, in contrast to its absence in the parent nitrile imine and *C*-methyl nitrile imine, may be due to the *p*-electron-donating effect of the NH₂ group, which is known to dramatically enhance the stability of carbene species.^[42] Indeed, the low lone-pair population on the amino nitrogen (0.70*e*) and high H₂N–C bond order (1.31) seem to reflect this *p*-electron-donating effect.

436 **Conclusions**

5-Aminotetrazole (**1**) was sublimated at 330 K, and its vapors were isolated in an argon matrix at 15 K and characterized by IR spectroscopy. Under these experimental conditions only the 2*H*-tautomeric form **1''** was found in the samples, in agreement with the theoretical predictions of the relative energies of isomers of **1**. Photolysis of **1''** in an argon matrix at $\lambda = 220$ nm allowed the capture of the *C*-amino nitrile imine **2** as the primary photoproduct. The identification of **2** as the *C*-amino nitrile imine was unequivocally confirmed by its IR spectrum, which was characterized in detail during subsequent photochemical experiments at $\lambda = 330$ nm. These experiments also revealed two different pathways for the photochemistry of the *C*-amino nitrile imine **2**: (1) Isomerization to the corresponding three-membered-ring 1*H*-diazirine **4** (which rearranges to carbodiimide **5**) and (2) decomposition to methylenimine **3** (which gives hydrogen isocyanide **6**). The observed isomerization route to 1*H*-diazirine **4** confirms the findings of our previous investigations on other nitrile imines,^[16,23] whereas the decomposition route to methylenimine **3** is reported here for the first time. We hypothesize that the carbenic character of **2** is crucial to open up the decomposition pathway to **3**, because it can be expected to increase the negative charge at the C atom to which the hydrogen atom migrates in the first stage of the decomposition process.

The experimental frequency of the $\nu_{\text{as}}(\text{CNN})$ mode of the *C*-amino nitrile imine **2** at 1998 cm⁻¹ stands apart from other nitrile imines (one of the lowest values observed so far), which indicates that **2** should have considerable carbenic character. This was corroborated by the calculated optimized geometry of the molecule, particularly when compared with those of the parent nitrile imine and the *C*-methyl-substituted derivative. This conclusion is supported by the analysis of the electronic structure using natural resonance theory (NRT), which shows that **2** has a contribution of around 20% of the carbenic resonance hybrid, contrasting with its absence in the parent nitrile imine and

the *C*-methyl nitrile imine (which can be described only by contributions of propargylic and allenic resonance hybrids). The *p*-electron-donating effect of the NH₂ group is most likely the key to the carbenic character of the *C*-amino nitrile imine **2**. 476

The quest for carbenic nitrile imines has been an almost unexplored topic. Our results demonstrate that the *C*-amino nitrile imine **2** has significant carbenic character, yet not to a point at which it could be considered a predominantly carbenic nitrile imine. Further studies with different substitution models need to be carried out to ultimately generate nitrile imines with dominant carbenic structure. This knowledge may lead to the synthesis of stable carbenic nitrile imines and the discovery of a new reactivity pattern for this 1,3-dipolar species. 481 486

Experimental Section

Sample: A commercial sample of 5-aminotetrazole (**1**; TCI Europe, 98%) was used. 491

Matrix Isolation IR Spectroscopy: To prepare low-temperature matrices, a solid sample of 5-aminotetrazole (**1**) was sublimated (at ca. 330 K) by using a miniature glass oven connected to the vacuum chamber of a cryostat. The vapors of **1** were co-deposited with a large excess of argon (N60, Air Liquide) onto a CsI window cooled to 15 K. The temperature of the CsI window was measured directly by a silicon diode sensor connected to a digital controller providing stabilization accuracy of 0.1 K. A closed-cycle helium refrigeration system was used in the experiments. The IR spectra were recorded with a resolution of 0.5 cm⁻¹ by using a Nicolet 6700 FTIR spectrometer equipped with a deuterated triglycine sulfate (DTGS) detector and a Ge/KBr beam splitter. To avoid interference from atmospheric H₂O and CO₂, the sample compartment of the spectrometer was modified to accommodate the cryostat head and allow purging of the instrument by a stream of dry air. 496 501 506

UV Laser Irradiation Experiments: The matrices were irradiated through an outer quartz window of the cryostat by using a tunable narrow-band frequency-doubled signal beam provided by an optical parametric oscillator (fwhm ≈ 0.2 cm⁻¹, repetition rate = 10 Hz, pulse energy ≈ 1 –3 mJ, duration = 10 ns) pumped with a pulsed Nd:YAG laser. 511

Theoretical Calculations: Calculations at the DFT and CCSD(T) levels of theory were performed as implemented in Gaussian 09^[43] and in GAMESS,^[44] respectively. Geometry optimizations followed by vibrational frequency calculations were performed at the B3LYP/6-311G++(d,p), CBS-QB3, and CCSD(T)/6-311++G(d,p) levels of theory. The nature of the stationary points was confirmed by analysis of the corresponding Hessian matrices. The harmonic vibrational frequencies calculated at the B3LYP/6-311++G(d,p) level of theory were scaled by 0.98 (below 3150 cm⁻¹) and by 0.950 (above 3150 cm⁻¹) to correct for vibrational anharmonicity, basis set truncation, and the neglected part of the electron correlation.^[45,46] The scaled frequencies together with the calculated IR intensities were then used to simulate the spectra by convoluting each peak with a Lorentzian function with a full width at half maximum (fwhm) of 1 cm⁻¹, and keeping the integral area of the simulated band equal to the theoretically calculated IR intensity.^[47] As a result of the broadening, the peak intensities of the simulated absorption bands are automatically reduced compared with the cal- 516 521 526

culated intensities (and then are shown in arbitrary units of “relative intensity”).

NBO and NRT Calculations: Bond orders and electron populations were calculated by the natural bond orbital (NBO) theory.^[48] NBO theory provides a representation of the molecular electronic configuration based on the classic localized Lewis bonding theory. It provides an amenable rationalization of the wavefunction obtained from electronic structure calculations in terms of Lewis bonding and antibonding orbitals as well as non-Lewis extra-valence Rydberg orbitals.^[49] The goal of the NBO algorithm was to find the idealized natural Lewis structure corresponding to the localized wavefunction $\Psi^{(L)}$ formed from doubly occupied Lewis-type NBOs. This is often inadequate for systems with strong electron delocalization, in which such effects appear as an average of multiple resonance structures α , as suggested by the original theory of Pauling and Wheland.^[50] In those systems, the localized density matrix $D^{(L)}$ is not a suitable approximation to the true delocalized density matrix $D^{(true)}$. Natural resonance theory (NRT) applies the resonance concept building on the general NBO method,^[49,51–53] searching for the best set of a number of localized resonance structure wavefunctions $\Psi_{\alpha}^{(L)}$ and associated localized density matrices $D_{\alpha}^{(L)}$ that can be weight-averaged by w_{α} to represent the true delocalized density matrix $D^{(true)}$ [Equation (1)]

$$D^{(true)} = \sum_{\alpha} w_{\alpha} D_{\alpha}^{(L)} \quad (1)$$

Therefore, in the light of NRT theory, a molecule under study can be regarded as a set of resonance hybrids that can be decomposed into a weighted set of resonance structures. The electronic structure analysis of nitrile imines was carried out with this methodology and by using the wavefunctions of fully optimized geometries obtained at the CCSD(T)/6-311++G(d,p) and B3LYP/6-311++G(d,p) levels of theory. ■■ ((=AUTHOR: Changes to ok?)) ■■

561 Acknowledgments

This work was supported by the Portuguese Fundação para a Ciência e a Tecnologia (FCT), ????? (FEDER) (via project PTDC/QUI-QUI/118078/2010, FCOMP-01-0124-FEDER-021082), and co-funded by ????? (QREN-COMPETE-UE). ■■ ((=AUTHOR: Please add full sponsor names!)) ■■ C. M. N. and I. R. acknowledge the FCT for a Postdoctoral Grant (No. SFRH/BPD/86021/2012) and an Investigador FCT grant, respectively. The Coimbra Chemistry Centre is also supported by the FCT through the project Pest-OE/UI0313/2014. Joel P. Ferreira is acknowledged for the assistance in experiments. Note: The authors declare no competing financial interest.

- [1] A. Padwa, W. A. Pearson (Eds.), *Synthetic Applications of 1,3-Dipolar Cycloaddition Chemistry Toward Heterocycles and Natural Products*, Wiley, New York, **2002**.
- [2] A. Padwa (Ed.), *1,3-Dipolar Cycloaddition Chemistry*, Wiley Interscience, New York, **1984**.
- [3] G. Wang, X. Liu, T. Huang, Y. Kuang, L. Lin, X. Feng, *Org. Lett.* **2013**, *15*, 76–79.
- [4] A. P. Antonchick, C. Gerding-Reimers, M. Catarinella, M. Schürmann, H. Preut, S. Ziegler, D. Rauh, H. Waldmann, *Nat. Chem.* **2010**, *2*, 735–740.
- [5] S. Filippone, E. E. Maroto, Á. Martín-Domenech, M. Suarez, N. Martín, *Nat. Chem.* **2009**, *1*, 578–582.
- [6] M. A. Tasdelen, Y. Yagci, *Angew. Chem. Int. Ed.* **2013**, *52*, 5930–5938; *Angew. Chem.* **2013**, *125*, 6044.

- [7] R. K. V. Lim, Q. Lin, *Acc. Chem. Res.* **2011**, *44*, 828–839.
- [8] Z. Yu, T. Y. Ohulchanskyy, P. An, P. N. Prasad, Q. Lin, *J. Am. Chem. Soc.* **2013**, *135*, 16766–16769.
- [9] Y. Wang, W. Song, W. J. Hu, Q. Lin, *Angew. Chem. Int. Ed.* **2009**, *48*, 5330–5333; *Angew. Chem.* **2009**, *121*, 5434. 591
- [10] W. Song, Y. Wang, W. J. Hu, Q. Lin, *J. Am. Chem. Soc.* **2008**, *130*, 9654–9655.
- [11] W. Song, Y. Wang, J. Qu, M. M. Madden, Q. Lin, *Angew. Chem. Int. Ed.* **2008**, *47*, 2832–2835; *Angew. Chem.* **2008**, *120*, 2874. 596
- [12] M. Alvaro, P. Atienzar, P. de la Cruz, J. L. Delgado, H. Garcia, F. J. Langa, *J. Phys. Chem. B* **2004**, *108*, 12691–12697.
- [13] B. Braida, C. Walter, B. Engels, P. C. Hiberty, *J. Am. Chem. Soc.* **2010**, *132*, 7631–7637.
- [14] D. H. Ess, K. N. Houk, *J. Am. Chem. Soc.* **2008**, *130*, 10187–10198. 601
- [15] A. S. Shawali, *Chem. Rev.* **1993**, *93*, 2731–2777.
- [16] a) We recently discovered a 1,3-dipolar species, the C-phenyl nitrile imine (Ph–CNN–H), that co-exists in two different structures corresponding to different energy minima (see ref.^[16b]); b) C. M. Nunes, I. Reva, R. Fausto, D. Bégué, C. Wentrup, *Chem. Commun.* **2015**, DOI: 10.1039/c5cc03518j. ■■ ((=AUTHOR: Are page numbers available?)) ■■ 606
- [17] D. Bégué, G. G. Qiao, C. Wentrup, *J. Am. Chem. Soc.* **2012**, *134*, 5339–5350. 611
- [18] G. Bertrand, C. Wentrup, *Angew. Chem. Int. Ed. Engl.* **1994**, *33*, 527–545; *Angew. Chem.* **1994**, *106*, 549.
- [19] M. Wong, C. Wentrup, *J. Am. Chem. Soc.* **1993**, *115*, 7743. ■■ ((=AUTHOR: Please give page range!)) ■■
- [20] R. C. Mawhinney, H. M. Muchall, G. H. Peslherbe, *Chem. Commun.* **2004**, 1862–1863. 616
- [21] F. Cargnoni, G. Molteni, D. L. Cooper, M. Raimondi, A. Ponti, *Chem. Commun.* **2006**, 1030–1032.
- [22] L. M. T. Frija, M. L. S. Cristiano, A. Gómez-Zavaglia, I. Reva, R. Fausto, *J. Photochem. Photobiol. C: Photochem. Rev.* **2014**, *18*, 71–90. ■■ ((=AUTHOR: Please check year and volume!)) ■■ 621
- [23] C. M. Nunes, C. Araujo-Andrade, R. Fausto, I. Reva, *J. Org. Chem.* **2014**, *79*, 3641–3646.
- [24] E. G. Baskir, D. N. Platonov, Y. V. Tomilov, O. M. Nefedov, *Mendeleev Commun.* **2014**, *24*, 197–200. 626
- [25] M. Pagacz-Kostrzewska, J. Krupa, M. Wierzejewska, *J. Phys. Chem. A* **2014**, *118*, 2072–2082.
- [26] M. Pagacz-Kostrzewska, J. Krupa, M. Wierzejewska, *J. Photochem. Photobiol. A: Chem.* **2014**, *277*, 37–44. 631
- [27] M. Pagacz-Kostrzewska, M. Mucha, M. Weselski, M. Wierzejewska, *J. Photochem. Photobiol. A: Chem.* **2013**, *251*, 118–127.
- [28] G. Maier, J. Eckwert, A. Bothur, H. P. Reisenauer, C. Schmidt, *Liebigs Ann.* **1996**, 1041–1053.
- [29] H. M. Muchall, *J. Phys. Chem. A* **2011**, *115*, 13694–13705. 636
- [30] D. Bégué, C. Wentrup, *J. Org. Chem.* **2014**, *79*, 1418–1426.
- [31] Bégué and Wentrup have investigated theoretically different amino-, hydroxy-, and fluoro-substituted nitrile imines, and found that heteroatom substituents with a lone pair stabilize the corresponding carbenic resonance structure of nitrile imines (see ref.^[30]). However, the experimental study of C-fluoro nitrile imines was not possible because of the lack of synthetic methods for preparing the corresponding 5-fluoro-tetrazoles (tetrazoles are precursors used to generate nitrile imines). 641
- [32] a) In agreement with what could be expected based on calculated relative energies for different tautomers of 5-aminotetrazole (1) discussed in the section “Tautomeric Equilibria in 5-Monosubstituted Tetrazoles” (Table 1). The 2*H* tautomer 1' was also found to be the most stable form in the gas phase and the major or exclusive form deposited in the matrix in several 5-monsubstituted tetrazoles, such as 5-methyl-, 5-phenyl-, and 5-chlorotetrazole (see refs.^[16,23,32b]); b) S. C. S. Bugalho, A. C. Serra, L. Lapinski, M. L. S. Cristiano, R. Fausto, *Phys. Chem. Chem. Phys.* **2002**, *4*, 1725–1731. 651 656

FULL PAPER

C. M. Nunes, I. Reva, M. T. S. Rosado, R. Fausto

- [33] It was observed that the photochemistry of **1'** only occurs with irradiation with $\lambda \leq 260$ nm, also in accord with the UV/Vis spectrum of 5-aminotetrazole (**1**; Figure S2 in the Supporting Information).
- 661 [34] Our optical parametric oscillator, with a frequency doubling option, has an intrinsic blind spot in the 370–340 nm region. Because of this, irradiation experiments were not carried out in this frequency range.
- 666 [35] M. E. Jacox, D. E. Milligan, *J. Mol. Spectrosc.* **1975**, 54–58, 333–356.
- [36] D. E. Milligan, M. E. Jacox, *J. Chem. Phys.* **1963**, 39, 712–715.
- [37] Scaled B3LYP/6–311++G(d,p) frequencies for the HNC molecule were estimated at 3617 [$\nu(\text{NH})$], 2053 [$\nu(\text{NC})$], and 484 [$\delta(\text{HCN})$] cm^{-1} .
- 671 [38] R. A. Seburg, R. J. McMahon, *J. Am. Chem. Soc.* **1992**, 114, 7183–7189.
- [39] H. Tomioka, N. Ichikawa, K. Komatsu, *J. Am. Chem. Soc.* **1992**, 114, 8045–8053.
- 676 [40] P. R. Schreiner, H. P. Reisenauer, F. C. Pickard, A. C. Simonett, W. D. Allen, E. Mátyus, A. G. Császár, *Nature* **2008**, 453, 906–909.
- [41] These species were also selected, because they were previously produced in low-temperature matrices (see refs.^[23,28]), and the experimental frequencies of the $\nu_{\text{as}}(\text{CNN})$ mode could be used as complementary information on their structures.
- 681 [42] G. Bertrand, “Stable Singlet Carbenes” in *Reactive Intermediate Chemistry* (Eds.: R. A. Moss, M. S. Platz, M. J. Jones), Wiley, ■■■ ((=<=AUTHOR: Location?)) ■■■, **2004**, pp. 329–373.
- 686 [43] M. J. Frisch, G. W. Trucks, H. B. Schlegel, G. E. Scuseria, M. A. Robb, J. R. Cheeseman, G. Scalmani, V. Barone, B. Mennucci, G. A. Petersson, H. Nakatsuji, M. Caricato, X. Li, H. P. Hratchian, A. F. Izmaylov, J. Bloino, G. Zheng, J. L. Sonnenberg, M. Hada, M. Ehara, K. Toyota, R. Fukuda, J. Hasegawa, M. Ishida, T. Nakajima, Y. Honda, O. Kitao, H. Nakai, T. Vreven, J. A. Montgomery Jr., J. E. Peralta, F. Ogliaro, M. Bearpark, J. J. Heyd, E. Brothers, K. N. Kudin, V. N. Starov-
erov, R. Kobayashi, J. Normand, K. Raghavachari, A. Rendell, J. C. Burant, S. S. Iyengar, J. Tomasi, M. Cossi, N. Rega, J. M. Millam, M. Klene, J. E. Knox, J. B. Cross, V. Bakken, C. Adamo, J. Jaramillo, R. Gomperts, R. E. Stratmann, O. Yazyev, A. J. Austin, R. Cammi, C. Pomelli, J. W. Ochterski, R. L. Martin, K. Morokuma, V. G. Zakrzewski, G. A. Voth, P. Salvador, J. J. Dannenberg, S. Dapprich, A. D. Daniels, Ö. Farkas, J. B. Foresman, J. V. Ortiz, J. Cioslowski, D. J. Fox, *Gaussian 09*, revision D.01, Gaussian, Inc., Wallingford, CT, **2009**.
- [44] M. W. Schmidt, K. K. Baldrige, J. A. Boatz, S. T. Elbert, M. S. Gordon, J. H. Jensen, S. Koseki, N. Matsunaga, K. A. Nguyen, S. Su, T. L. Windus, M. Dupuis, J. A. Montgomery, *J. Comput. Chem.* **1993**, 14, 1347–1363.
- [45] C. M. Nunes, I. Reva, T. M. V. D. Pinho e Melo, R. Fausto, *J. Org. Chem.* **2012**, 77, 8723–8732.
- [46] C. M. Nunes, I. Reva, T. M. V. D. Pinho e Melo, R. Fausto, T. Solomek, T. Bally, *J. Am. Chem. Soc.* **2011**, 133, 18911–18923.
- [47] K. K. Irikura, *Program SYNSPEC*, National Institute of Standards and Technology, Gaithersburg, MD, **2009** ■■■ ((=<=AUTHOR: Year ok?)) ■■■.
- [48] E. D. Glendening, J. K. Badenhoop, A. E. Reed, J. E. Carpenter, J. A. Bohmann, C. M. Morales, F. Weinhold, *NBO 5.0*, Theoretical Chemistry Institute, University of Wisconsin, Madison, WI, **2001**.
- [49] F. Weinhold, C. R. Landis, *Valency and Bonding: A Natural Bond Orbital Donor-Acceptor Perspective*, Cambridge University Press, Cambridge, **2005**.
- [50] L. Pauling, *The Nature of the Chemical Bond and the Structure of Molecules and Crystals: An Introduction to Modern Structural Chemistry*, Cornell University Press, Ithaca, NY, **1960**.
- [51] E. D. Glendening, F. Weinhold, *J. Comput. Chem.* **1998**, 19, 593–609.
- [52] E. D. Glendening, F. Weinhold, *J. Comput. Chem.* **1998**, 19, 610–627.
- [53] E. D. Glendening, J. K. Badenhoop, F. Weinhold, *J. Comput. Chem.* **1998**, 19, 628–646.

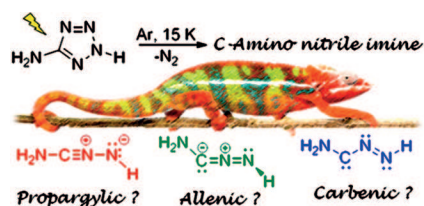
Received: September 4, 2015

731


A C-Amino nitrile imine has been generated in a low-temperature matrix. Experimental and computational characterization has demonstrated that the C-amino nitrile imine has significant carbenic character. These results pave the way to the discovery of carbenic nitrile imines.

736

741



C. M. Nunes,* I. Reva, M. T. S. Rosado,
R. Fausto 1–11

The Quest for Carbenic Nitrile Imines: Experimental and Computational Characterization of a C-Amino Nitrile Imine 

Keywords: Nitrile imines / Structure elucidation / Matrix isolation / Photochemistry / Density functional calculations

746

Authors: Please check that the ORCID identifiers listed below are correct. We encourage all authors to provide an ORCID identifier for each coauthor. ORCID is a registry that provides researchers with a unique digital identifier. Some funding agencies recommend or even require the inclusion of ORCID IDs in all published articles, and authors should consult their funding agency guidelines for details. Registration is easy and free; for further information, see <http://orcid.org/>.

751

Cláudio M. Nunes <http://orcid.org/0000-0002-8511-1230>*
Igor Reva <http://orcid.org/0000-0001-5983-7743>
Mário T. S. Rosado <http://orcid.org/0000-0001-5782-8819>
Rui Fausto <http://orcid.org/0000-0002-8264-6854>